HHS Public Access

Author manuscript

Matrix Biol. Author manuscript; available in PMC 2017 May 01.

Published in final edited form as:

Matrix Biol. 2016 ; 52-54: 162–175. doi:10.1016/j.matbio.2016.02.010.

PTH Signaling Mediates Perilacunar Remodeling During Exercise

Joseph D. Gardinier[a,b], **Salam Al-Omaishi**[c], **Michael D. Morris**[d], and **David H. Kohn**[b,c]

[a]Bone and Joint Center, Henry Ford Hospital, Detroit, MI, 48202 USA

[b]Department of Biologic and Materials Sciences, University of Michigan, Ann Arbor, MI, 48109 USA

[c]Department of Biomedical Engineering, University of Michigan, Ann Arbor, MI, 48109 USA

[d]Department of Chemistry, University of Michigan, Ann Arbor, MI, 48109 USA

Abstract

Mechanical loading and release of endogenous parathyroid hormone (PTH) during exercise facilitate the adaptation of bone. However, it remains unclear how exercise and PTH influence the composition of bone and how exercise and PTH-mediated compositional changes influence the mechanical properties of bone. Thus, the primary purpose of this study was to establish compositional changes within osteocytes' perilacunar region of cortical bone following exercise, and evaluate the influence of endogenous PTH signaling on this perilacunar adaptation. Raman spectroscopy, Scanning electron microscopy (SEM), and Energy Dispersive X-ray Spectroscopy (EDS) were used to evaluate tissue composition surrounding individual lacuna within the tibia of 19 week old male mice exposed to treadmill running for 3 weeks. As a result of exercise, tissue within the perilacunar region (within 0–5 μm of the lacuna wall) had a lower Mineral-to-Matrix Ratio (MMR) compared to sedentary controls. In addition, exercise also increased the Carbonate-to-Phosphate Ratio (CPR) across both perilacunar and non-perilacunar regions (5–10 μm and 10–15 μm from the lacuna walls). Tibial post-yield work had a significant negative correlation with perilacunar MMR. Inhibition of PTH activity with PTH(7–34) demonstrated that perilacunar remodeling during exercise was dependent on the cellular response to endogenous PTH. The osteocytes' response to endogenous PTH during exercise was characterized by a significant reduction in SOST expression and significant increase in FGF-23 expression. The potential reduction in phosphate levels due to FGF-23 expression may explain the increase in carbonate substitution. Overall, this is the first study to demonstrate that adaptation in tissue composition is localized around individual osteocytes, may contribute to the changes in whole bone mechanics during exercise, and that PTH signaling during exercise contributes to these adaptations.

Corresponding Author: David H. Kohn, Ph.D., Dept. of Biological and Material Sciences, 2213 School of Dentistry, University of Michigan, Ann Arbor, MI 48109-1078, (tel) 734-764-2206, ; Email: dhkohn@umich.edu.

Keywords

Raman spectroscopy; Exercise; Parathyroid Hormone; Perilacunar Remodeling; Osteocyte

Introduction

Bone is a complex living tissue with the unique ability to model and remodel its structure and mechanical properties to support sustained loads. As a composite structure, the mechanical properties of bone are influenced by its composition and spatial distribution (Boskey et al., 1999; Burstein et al., 1975). Modeling and remodeling of bone tightly regulate its composition and distribution to optimize mechanical properties (Robling et al., 2006). Although extensive work has identified cellular mechanisms that promote bone formation and remodeling, the impact of many of these signaling pathways on the mechanical properties of bone remains unclear. Understanding how mechanisms at the cellular level influence tissue composition and distribution of bone at the matrix-level, and also the mechanical properties of bone at the tissue and whole bone-levels, is vital for developing treatments that improve bone quality.

Bone quality can improve in response to various forms of exercise. There is an increase in bone metabolism in humans at the onset of exercise (Maimoun and Sultan, 2009; Scott et al., 2011) that is followed by an increase in bone mineral content (Wallace and Cumming, 2000). However, there is limited understanding of how exercise influences the mechanical properties of bone, given that increased mineral content or bone quantity does not always translate into improved mechanical function (Hui et al., 1988). To this end, animal studies have identified structural and tissue-level mechanical properties that increase during various forms of exercise, such as swimming, jumping, voluntary running in a cage wheel or running on a treadmill (Gardinier et al., 2015; Hoshi et al., 1998; Huang et al., 2003; Iwamoto et al., 2004; Iwamoto et al., 1999; Kohn et al., 2009). For example, young adult mice running on a treadmill consistently exhibit increased structural and tissue-level properties, such as post-yield properties of the tibia (Gardinier et al., 2015; Hoshi et al., 1998; McNerny et al., 2015; Wallace et al., 2010; Wallace et al., 2009). Both structural and tissue-level properties can increase following exercise despite no significant changes in size, geometry, or mineral content (Gardinier et al., 2015; Kohn et al., 2009). However, investigation of tissue composition reveals increased carbonate-to-phosphate ratio, mineral-to-matrix ratio, and ratio of mature to immature collagen cross-links that correspond with strength and post-yield displacement gained during exercise (Kohn et al., 2009; Wallace et al., 2010), Given that these findings represent a global average taken across the entire intracortical region, it remains unclear where these compositional changes are localized or where they may originate from, both of which are vital towards understanding how bone optimizes its strength without altering its shape and size.

The mechanical properties, mineral composition, and collagen cross-links that increase with exercise are considered a function of the dynamic loading and changes in calcitropic hormones that invoke specific cellular responses. In particular, we have demonstrated that the cellular response to endogenous parathyroid hormone (PTH) released during exercise

facilitates an increase in stiffness and post-yield displacement, and reduction in yield displacement compared to sedentary controls (Gardinier et al., 2015). Although PTH and mechanical loading are primarily associated with increased bone formation, both forms of stimuli also cause structural changes in the lacuna-canaliculi system of cortical bone (Blaber et al., 2013; Britz et al., 2012; Qing and Bonewald, 2009). In response to PTH, or in the absence of mechanical loads during spaceflight, lacunae volume can increase significantly (Blaber et al., 2013; Qing et al., 2012). Lactation similarly increases lacuna size, mediated by the calcitonin receptor (Clarke et al., 2015), as well as the osteocytes' response to PTH (Qing et al., 2012). This enlargement of the lacuna is often referred to as 'osteocytic osteolysis' (Qing and Bonewald, 2009), and can be counteracted by the addition of new tissue (Sano et al., 2015). This local remodeling is indicative of the osteocytes' ability to not only alter the lacuna structure, but also modify the mass density and chemical composition of the perilacunar tissue (Hesse et al., 2014).

To facilitate perilacunar remodeling, osteocytes can dissolve the surrounding mineral to enlarge their lacuna space by increasing acidity and degrading the mineral and matrix through tartrate-resistant acid phosphatase (TRAP), cathepsin-k (Ctsk), carbonic anhydrase 2 (CaII), and matrix metalloproteinase (MMP) activity (Holmbeck et al., 2005; Kogawa et al., 2013; Nyman et al., 2011; Qing et al., 2012; Tang et al., 2012). In osteocyte-specific PTH/PTH-related protein receptor knockout mice, inhibition of lacuna enlargement and TRAP expression was observed during lactation (Clarke et al., 2015; Qing et al., 2012). With regards to the matrix, osteocyte expression of MMPs allows the lacuna and canaliculi structure to be maintained, while the loss of MMP expression leads to a decrease in mechanical properties of bone, specifically whole bone stiffness, strength, and modulus (Nyman et al., 2011; Tang et al., 2012). Replacing the mineral or matrix in the perilacunar zone is less understood. Given the similarities to osteoblasts, osteocytes have the capacity to generate alkaline phosphate (ALP) and type-1 collagen (COL1), along with other non-collagenous proteins (Bonewald, 2011). As a result, osteocytes have the capacity to alter the mineral or matrix composition, such that the structural and/or tissue-level mechanical properties of bone are affected without requiring global changes to bone size or geometry.

We therefore hypothesized that endogenous PTH signaling during exercise mediates changes in the perilacunar tissue composition, and that this perilacunar adaptation contributes to the mechanical property changes that result from exercise. The purpose of this study was to: (1) establish that changes in perilacunar composition occur following short-term exercise, and (2) demonstrate the influence endogenous PTH signaling has on perilacunar adaptation during exercise.

Results

2.1 Perilacunar Tissue Composition is Altered During Exercise

Compared to sedentary controls, the exercise group exhibited a significantly smaller mineral-to-matrix ratio (MMR) within the perilacunar region (0 to 5 microns from the lacuna wall), but not in either non-perilacunar region (5 to 10, and 10 to 15 microns from the lacuna wall) (Fig 1). The exercise group also exhibited a significantly greater carbonate-to-phosphate ratio (CPR) compared to sedentary controls across both perilacunar and non-

perilacunar regions. This increase in CPR indicates a more carbonated apatite throughout the bone of mice subjected to exercise.

Inhibition of the cellular response to endogenous PTH was achieved by treating mice with PTH(7–34) during both exercise and sedentary conditions. Perilacunar MMR was not significantly different between exercise and sedentary groups treated with PTH(7–34). The CPR in the perilacunar and non-perilacunar regions were also not significantly different between exercise and sedentary groups treated wtih PTH(7–34). These data indicate that the cellular response to endogenous PTH released during exercise is necessary for the decrease in the perilacunar MMR and increase in the CPR across both perilacunar and non-perilacunar tissue.

To substantiate the Raman data, the mineral density and elemental composition surrounding individual lacuna were measured using backscatter electron (BSE) scanning electron microscopy along with energy dispersive X-ray spectroscopy (EDS). Based on normalized grey-scale values, the mineral density immediately next to the lacuna wall (0 to 2.5 microns away) was significantly higher compared to non-perilacunar tissue in sedentary controls ($p < 0.01$; Fig 2). However, mineral density next to the lacuna wall was significantly smaller in the exercise group compared to the non-perilacunar tissue and also compared to the perilacunar tissue in sedentary controls ($p < 0.01$ for both comparisons). The elemental carbon-to-phosphorus ratio (ECPR) was significantly higher ($p < 0.01$) across each region in the exercise group compared to sedentary controls, indicating either a decrease in the carbon content or increase in phosphorus. By inhibiting the cellular response to endogenous PTH with PTH(7–34), there was no longer a differential in perilacunar mineral density and ECPR between exercised and sedentary groups.

2.2 Post-Yield Properties Gained During Exercise are Regulated By PTH Signaling and Correspond With Perilacunar Remodeling

As reported in our previous study (Gardinier et al., 2015), tibiae from the exercise group had a significantly smaller yield displacement in the tibia along with a significantly greater stiffness and post-yield work compared to sedentary controls (Table 1). The tissue-level mechanical properties of the tibia demonstrated similar trends, with a significant decrease in yield-strain, but significant increases in modulus and ultimate stress compared to sedentary controls. Adaptations in the mechanical properties of the tibia as a result of exercise were not accompanied by any changes in cortical area, mineral density, mineral content, or moment of inertia when compared to sedentary controls (Table 2). Inhibiting the cellular response to endogenous PTH with PTH(7–34) inhibited the increase in stiffness and post-yield work, and decrease in yield-displacement in exercised mice compared to sedentary controls. However, PTH(7–34) treatment did not inhibit exercise from increasing the modulus, ultimate stress, or decreasing the yield-strain when compared to sedentary controls. Therefore, the structural-level mechanical properties gained during exercise are dependent on PTH signaling. There was a significant negative correlation between the MMR and post-yield work (Fig 3A). The increase in post-yield work following exercise was dependent on the cellular response to endogenous PTH signaling (Fig 3B).

2.3 Endogenous PTH Signaling During Exercise Contributes to Tissue Resorption and Increases in Osteocyte Signaling

To evaluate osteocytes' ability to mediate perilacunar remodeling during exercise, gene expression in osteocyte-rich tibiae was measured during the first week of the exercise program. There was a significant decrease in Sclerostin gene (SOST) expression by day 2 in exercised mice compared to sedentary controls (0.35 ± 0.08 vs. 1.0 ± 0.23, p-value = 0.01), but this decrease was lost by day 4 (Fig 4A) and then regained on day 6 (Fig 4B). Prior to day 6, exercise did not affect fibroblast growth-factor 23 (FGF-23) expression, but after 6 days, FGF-23 expression was ~ 3.5 fold greater in exercised mice than sedentary controls. Expression levels of MT1-MMP and TRAP were increased by 4 days of exercise when compared to sedentary conditions, but only MT1-MMP was statistically significant compared to sedentary controls. However, by day 6, exercised mice exhibited a significant decrease in both MT1-MMP and TRAP compared to sedentary controls. Expression levels of COL1A2 and ALP were not significantly different between exercise and sedentary conditions at any of these times (Supplementary Fig 1).

At day 4, the increase in MT1-MMP and TRAP due to exercise was inhibited by PTH(7–34) treatment when compared to sedentary controls (Fig 4A). By day 6, the decrease in MT1-MMP and SOST along with the increase in FGF-23 due to exercise was inhibited by PTH(7–34) when compared to sedentary controls (Fig 4B). Although FGF-23 was higher following exercise + PTH(7–34), it was not significantly different from sedentary mice treated with PTH(7–34).

2.4 Marginal Changes in Lacuna Size During Exercise

Alongside the changes in tissue composition, lacuna volume was expected to shift as result of perilacunar adaptation and local tissue formation or resorption. In response to exercise, lacuna area was greater compared to sedentary controls; however this increase was not statistically significant. Lacuna size did not correlate with the MMR ($R^2 = 0.011$, p-value = 0.32); however, there was a positive correlation with CPR ($R^2 = 0.046$, p-value < 0.05), meaning that larger lacuna tend to have a higher CPR.

Discussion

The endogenous PTH released in mice while running on a treadmill facilitates adaptation in tissue composition of the tibia that is localized 0 to 5 microns from the lacuna wall (Fig 1 & 2). These changes in composition are not detected over larger regions of tissue (Supplemental Fig 2). Within this perilacunar region, the mineral had higher carbonate substitution, but decreased mineral density, along with a decrease in the mineral to organic matrix ratio. The increase in carbonate substitution may explain the increased stiffness measured at the whole bone level (Table 1), while the reduction in mineral-to-matrix ratio correlated with the corresponding increase in post-yield properties of the tibia (Fig 3). This exercise model increased structural-level mechanical properties in the tibia of young adult mice without altering its cross-sectional area or geometry (Table 2), consistent with other studies using this model (Gardinier et al., 2015; Kohn et al., 2009). Together, these data demonstrate that the structural-level properties gained during exercise correspond with

localized changes in tissue composition without requiring significant changes in cortical bone size or geometry. In addition, we have established that the cellular response to endogenous PTH released during running is a dominant stimulus for tissue adaptation that is localized at the lacuna wall.

The mechanical behavior of bone, specifically tissue strength and stiffness, is largely determined by its degree of mineralization (Burstein et al., 1975). Although exercise increased the stiffness and modulus of the tibia (Table 1), the MMR exhibited no significant changes in non-perilacunar regions compared to sedentary controls, while the perilacunar MMR was significantly reduced (Fig 1). A reduction in MMR would suggest either demineralization in the perilacunar region, which would decrease tissue stiffness and strength (Burstein et al., 1975), or an increase in matrix formation, which would increase tissue ductility (Boskey et al., 1999). The organic matrix in bone is a key determinant of its post-yield properties (Boskey et al., 1999), and we found a negative correlation between perilacunar MMR and post-yield work (Fig. 4B). Under bending, cracks often originate and propagate through the lacunae-canaliculi system (Reilly, 2000). Therefore, modifying the organic matrix or mineral density within the perilacunar region may influence the work or energy the bone can sustain.

Beyond the degree of mineralization, bone mineral stoichiometry and crystallinity also contribute to its mechanical function, particularly strength and stiffness (Boskey, 2003; Morris and Mandair, 2011). The mineral phase of bone is comprised of hydroxyapatite crystals, where carbonate substitution into the lattice occurs with maturation of the mineral (Akkus et al., 2004; Raghavan et al., 2012). Exercise increased the CPR throughout the cortical bone of the tibia, with the largest increase occurring at the lacuna wall (Fig. 1). The overall increase in CPR across perilacunar and non-perilacunar regions is consistent with previous studies demonstrating an increase in CPR across the bulk of the tissue (Wallace et al., 2010). Although a more carbonated apatite is expected to provide a locally stiffer and possibly stronger material (Burket et al., 2011; de Carmejane et al., 2005; Donnelly et al., 2010), its ability to do so at the whole bone-level remains unclear. For example, sites of hip fracture in postmenopausal women have a higher CPR than neighboring undamaged sites (McCreadie et al., 2006), which would indicate that increased CPR occurs in weaker tissue. This is supported by observations that ovariectomized monkeys have a larger CPR along with weaker and more brittle tissue (Gadeleta et al., 2000). In contrast, areas of diffuse damage following repetitive loading tend to exhibit a less carbonated apatite (Timlin et al., 2000), suggesting that decreased CPR may be associated with weaker tissue. In addition to carbonate substitution, crystallinity is also a key determinant of the mechanical properties of the mineral, and often exhibits an inverse relationship with CPR (Boskey, 2003; Morris and Mandair, 2011; Raghavan et al., 2012). After exercise, the increase in CPR was accompanied by a decrease in crystallinity, specifically at the lacuna wall (Fig. 1). A decrease in crystallinity can occur from an expansion of the c-axis of the apatite crystal, resulting from carbonate substitution of the phosphate (Baig et al., 1999). Although the decrease in the perilacunar crystallinity following exercise was not statistically significant, earlier studies found significant decreases in crystallinity throughout the bone with exercise (Wallace et al., 2010).

It is hypothesized that the decreases in MMR measured with Raman and mineral density measured under BSE are due to mineral being removed from the perilacunar region following exercise. We therefore anticipated an increase in lacuna area with exercise, similar to that observed during lactation (Clarke et al., 2015; Qing et al., 2012). However, only a non-significant increase lacuna size occurred with exercise (Fig 5). Enlargement of lacuna volume during lactation is mediated by the activation of osteocytes' PTH/PTH-related protein receptor (Qing et al., 2012). To a similar degree, micro-gravity during spaceflight causes the lacuna to become enlarged, indicating that the absence of mechanical loading accelerates the removal of the perilacunar mineral (Blaber et al., 2013). In contrast, paralysis of the hind-limb decreases lacuna volume (Britz et al., 2012). Although the loss of muscle function and potential cross-talk with bone may contribute to the discrepancy between results from hind-limb suspension and other forms of unloading, it remains unclear how lacuna volume may change under mechanical loading. Based on our results, mechanical loading may induce enough tissue formation to replace the tissue removed in response to PTH, causing a net zero change in lacuna size.

Osteocytes' ability to mediate this adaptation in tissue composition was evaluated based on changes in gene expression. Analysis of osteocyte markers revealed a significant increase in FGF-23 and decrease in SOST by day 6 (Fig 4B). FGF-23, in particular, is found only in osteocytes, and plays a key role in regulating phosphate wasting within the kidney (Silver and Naveh-Many, 2013). The increase in FGF-23 after day 6 of exercise could cause an increase in phosphate wasting and a reduction the amount of phosphate circulating in the mice. In the process of new tissue being mineralized, the lack of available phosphate would likely result in a more carbonated apatite being formed. This could explain the decrease in CPR observed during exercise (Fig 1), similar to how hyperphosphotemia from chronic renal failure increases cortical bone CPR (Iwasaki et al., 2011). The potential use of FGF-23 to augment newly mineralized tissue after 6 days of exercise coincided with a decrease in SOST expression (Fig 4B). The subsequent decrease in Sclerostin would then reduce the osteocytes' catabolic activity or 'osteocytic osteolysis', given that Sclerostin activates TRAP and CaII expression needed to facilitate mineral dissolution (Kogawa et al., 2013). Thus, it would make sense that the decrease in SOST expression corresponded with a decrease in TRAP expression (Fig 4B). Altogether, the increase in FGF-23 expression alongside a decrease in SOST and TRAP expression suggests that after 6 days of exercise, osteocytes are reducing their catabolic behavior and are primed to increase carbonate substitution.

Prior to day 6, the catabolic function of osteocytes is difficult to clearly define. We observed an initial increase in MT1-MMP and TRAP expression by day 4 (Fig 4A). Although these proteins are not exclusive to osteocytes, they are used by osteocytes to maintain the lacunae-canaliculi system and have a large impact on whole bone mechanical properties (Nyman et al., 2011; Tang et al., 2012). The lack of changes in Col1 or ALP gene expression by day 4 (Suppl Fig 1), would also suggest the presence of more catabolic activity at the onset of exercise. The potential increase in catabolic activity is also consistent with the increase in lacuna size, even though it was not statistically significant (Fig 5A). The initial increase in catabolic activity among osteocytes may be offset by the subsequent reduction by day 6, based on osteocytes' expression of SOST along with the decrease in TRAP and MT1-MMP expression.

Osteocyte gene expression and perilacunar adaptation were both dependent on the cellular response to endogenous PTH released during exercise. The structural-level mechanical properties that increase with exercise are also dependent on the cellular response to the increase in endogenous PTH levels (Gardinier et al., 2015). While other studies have demonstrated increased tissue strength and post-yield behavior following 3 weeks of exercise, opposite trends in MMR and CPR were also found (Kohn et al., 2009; Wallace et al., 2010). However, the tissue composition reported in these earlier studies represented a global average across the entire cross-section that was based on individual measurements from larger regions of tissue, roughly 20 times greater than the perilacunar and nonperilacunar regions presented in this study. In a secondary analysis, the MMR and CPR were measured across a larger region expanding 0 to 20 microns away from the lacuna wall. The MMR and CPR across this larger region were not significantly different between exercise and sedentary groups (Supplementary Fig 2). As a result, localized variations in tissue composition are easily negated when taking measurements across larger portions of tissue. Our ability to assess MMR and CPR localized within 5 μm of the lacuna wall enabled us to identify tissue adaptation within the osteocytes' perilacunar region and its potential to alter the mechanical properties of bone.

One of the limitations in this study was the inability to completely avoid the presence of non-osteocytic cells when evaluating changes in gene expression. Although care was taken to remove the bone marrow and any remaining lining cells, as prescribed by established techniques (Kelly et al., 2014), the expression levels of MT1-MMP, TRAP, ALP and collagen are not osteocyte specific. However, SOST and FGF-23 are not expressed in other cells, and the changes in expression of these genes indicate that osteocytes play a key role in mediating bone adaptation during exercise and in response to endogenous PTH signaling.

This study is the first to establish the presence of perilacunar adaptation in response to exercise and demonstrate that endogenous PTH signaling during exercise mediates this adaptation. Based on our data, this perilacunar adaptation may facilitate changes in structural-level mechanical properties of the tibia, specifically post-yield properties. As a result, these data suggest that osteocytes may play a direct role in governing the mechanical properties of cortical bone.

Experimental Procedure

4.1 3-Week In-vivo Exercise Model

Animal procedures were performed at the University of Michigan with University Committee on Use and Care of Animals (UCUCA) approval. Male C57Bl/6J mice were purchased from Jackson Laboratories (ME) at the age of 15 weeks and were individually housed throughout the entire study (because of their aggressive nature) with sufficient water, food, and items for enrichment. Mice were allowed to acclimate for one week. At 16 weeks of age, they were divided into four weight-matched groups with 8 mice in each group: sedentary + vehicle, sedentary + PTH(7–34), exercise + vehicle, and exercise + PTH(7–34). Exercise groups were subjected to 30 minutes of running on a treadmill at 12 m/min and 5° incline for 21 consecutive days. Each day, mice received subcutaneous injections of a vehicle control (50μl of 0.9% saline) or 60μg/kg of PTH(7–34) to inhibit PTH signaling. On

day 22, each mouse was sacrificed and tibiae were removed, stripped of soft tissue, wrapped in gauze soaked with Ca^{2+} buffered saline and stored at −80°C. The left tibia was later scanned using micro-CT and then tested under mechanical loading to determine its mechanical properties. The right tibia was used to identify corresponding changes in tissue composition within the osteocytes' perilacunar region.

4.2 Micro-CT

Cortical bone mineral content, density, and cross-sectional geometry were determined from ex-vivo scans of the entire tibia using a Scanco microCT system (μCT100 Scanco Medical, Bassersdorf, Switzerland). Each tibia was embedded in 1% agarose, placed in a 19 mm diameter tube, and scanned with the following settings: 10 μm, voxel size, medium resolution, 70 kVp, 114 μA, 0.5 mm AL filter, integration time 500ms. Image slices were processed using the manufacturer's software and a single greyscale threshold, which was optimized between 0–1000 across all the samples. Cortical bone mineral content, mineral density and geometry (cortical area, moment of inertia) were quantified at a standard site, located 3 mm proximal of the tibia-fibula junction. To estimate the tissue-level mechanical properties, cortical bone area, moment of inertia about the medial-lateral axis, and the distance from the most medial point to the neutral axis was determined at the fracture site.

4.3 Mechanical Loading

The mechanical properties reported in this study represent a subset of tibia from our early study (Gardinier et al., 2015). Since perilacunar remodeling was only evaluated in this subset of tibia, we only included their mechanical properties. This also allowed us to run correlation studies between the mechanical properties and their respective properties in perilacunar remodeling. As described in our study, the mechanical properties were determined under four-point bending with a base support of 9 mm and loading points 3 mm apart. Each tibia was positioned in the loading device with the lateral surface under compression and the most distal portion of the tibia-fibula junction over the outer base support. Each sample was tested until failure at a loading rate of 0.01 mm/s (Admet eXpert Universal Testing Machine). The location of failure was noted, while load and deflection were recorded to quantify structural-level properties: yield-force, ultimate-force, yield-deformation, ultimate-deformation, failure load, failure displacement, stiffness, and strain-energy. Tissue-level mechanical properties were estimated using beam-bending equations along with the cross-sectional area, distance from the most lateral surface to the neutral-axis, and the moment of inertia (MOI) at the fracture site. The resulting stress-strain relationship provided yield-stress, ultimate-stress, yield-strain, ultimate-strain, and modulus. The mean and standard error for each group are reported.

4.4 Raman Spectroscopy and Lacuna Size

Tissue composition localized around individual lacuna was measured using Raman spectroscopy. Tibiae were first dehydrated in a graded ethonal (70%, 80%, 100%), then embedded in methyl methacrylate (Koldmount Cold Mount kit, Mager Scientific, MI). Sections 1 mm thick were cut at the mid-diaphysis with a diamond wafering blade (Mager Scientific, MI) on a low-speed sectioning saw (South Bay Technology, Model 650, CA) and then polished to a final thickness of 200 μm on wet silicon carbide abrasive disks. Each

section was imaged using a Raman microprobe with a line focused laser beam (135 to 180 μm in length) (Carden et al., 2003; Timlin et al., 2000). A 785-nm diode laser (Invictus, Kaiser Optical Systems) was focused through a 40X/0.75N objective (S Fluor, Nikon Instruments) on a motorized translation stage. Hyperspectral Raman images were taken at 3 distances from the lacuna wall: 0–5 μm, 5–10μm, and 10–15 μm. The region closet to the lacuna (0–5 μm) is referred to as the perilacunar region. Image data was processed using custom MATLAB scripts (Carden et al., 2003; Timlin et al., 2000), which normalized each image to the peak intensity of phosphate and then implemented a peak fitting routine to find peak intensities for phosphate (959 cm^{-1}), carbonate (1070 cm^{-1}), and the hydroxyprolines (851 cm^{-1} and 873 cm^{-1}) to represent the matrix phase. The carbonate-to-phosphate ratio (CPR) was defined 1070 cm^{-1}/958 cm^{-1}, and the mineral-to-matrix ratio (MMR) was defined as 959 cm^{-1}/(851 cm^{-1} and 873 cm^{-1}), while the crystallinity was calculated by taking the inverse of the phosphate band width at half of the maximum intensity (1/958 cm^{-1}, FWHM). The size of each lacuna assed under Raman was determined by outlining an image of each lacuna in Matlab and measuring its cross-sectional area. Each parameter was averaged across 3 to 4 imaged lacunae taken from the same sample. Each lacuna was selected from the medial aspect of the sample's transverse cross-section to correspond with the mechanical properties of contralateral limb, which was loaded with the medial aspect under tension. A total of 8 samples were tested for each group and the mean and standard error calculated for each group is reported.

4.5 SEM and EDS Imaging

Mineral density and the relative elemental abundance of phosphorous and carbon were evaluated using backscatter electron (BSE) imaging along with energy dispersive X-ray spectroscopy (EDS). Tibial sections were cut at the mid-diaphysis from previously embedded bones adjacent to those prepared for Raman. Each section was polished to a final thickness of 1 μm using silicon carbide abrasive disks followed by a 0.25 micron diamond suspension and then thinly coated with gold. A JEOL-7800FLV Scanning Electron Microscope with an integrated EDS detector was used to image each section under a 7×10^{-4} Pa vacuum and the electron beam energy was kept at 15 kV with an operating distance of 10 mm. To account for variations between each imaging session, BSE and EDS images were taken of a hydroxyapatite standard.

Digital images of individual lacuna and their surrounding tissue were captured first under BSE detection. For each BSE imaged lacuna, the mean grey-scale value was recorded within concentric regions every 2.5 microns, starting at the lacuna wall (Fig. 6). Each grey-value was normalized by the mean grey-value of the corresponding hydroxyapatite standard and then normalized by the non-perilacunar tissue furthest away from the same lacuna. For EDS analysis, spectra were taken every 2.5 microns along a line extending perpendicular from the lacuna wall. The elemental ratio between carbon and phosphorus was determined using AzTec Software and normalized to the hydroxyapatite standard imaged during the same session. For each tibia, the grey-scale value and carbon-to-phosphorus ratio within each region was averaged across 7 to 8 lacuna. Similar to the lacunae selected for Raman spectroscopy, each lacuna was selected from the medial aspect of the sample's transverse cross-section. The mean and standard error across the 8 tibia within each group are reported.

4.6 Initial Changes in Gene Expression During Exercise

Changes in gene expression were evaluated in response to exercise at different time points in a second batch of mice. Using the same genetic strain and gender, 16 week-old mice were divided into 5 groups: baseline, sedentary + vehicle, sedentary + PTH(7–34), exercise + vehicle, and exercise + PTH(7–34). Within each group, mice were divided into 3 different sub-groups that represented the number of days each mouse was subjected to exercise: 2 days, 4 days, and 6 days. Each sub-group was assigned 8 mice. Mice were exposed to the same exercise regimen and treatments described in the 3-week study. Once each mouse was treated according to their allotted time span, the mice were sacrifice, the tibiae were removed, cleaned of excess tissue along with their epiphysis and centrifuged to remove the bone marrow and lining cells as described (Kelly et al., 2014). Both tibiae were homogenized and mRNA was extracted using a Trizol extraction method. The mRNA was purified using an RNeasy® Mini Kit (Qiagen) and cDNA was generated with the Taqman cDNA synthesis kit (Applied Biosystems) according to the manufacturer's specifications. qRT-PCR was carried out using an Applied BioSystems 7500 RealTime PCR machine along with Taqman primers: RN18S (Mm03928990-g1), MT1-MMP (Mm00485054-m1), TRAP (Mm00475698-m1), COL1A1 (Mm00801666-g1), Alp (Mm00475831-m1), FGF-23 (Mm00445621-m1), and SOST (Mm00470479-m1). Gene expression for each sample was quantified based on a standard curve derived for each primer and then normalized by their respective RN18S expression. The mean and standard error was reported for each group.

4.7 Statistical Analysis

Raman, SEM, and EDS outcomes were tested for statistical differences in the same manner using SPSS software. Within each group, differences between spatial regions were tested using a one-way ANOVA, with a p-value < 0.05 indicating statistical significance. At each location, the effects of exercise and PTH(7–34) were tested using a two-way ANOVA, with a p-value < 0.05 indicating a significant difference. Student-Newman Keuls post hoc tests were employed to assess differences between sedentary and exercise groups along with the interactions between vehicle and PTH(7–34) treatments. Two-way ANOVA was also used to determine differences in mechanical properties between sedentary and exercise groups, along with the interactions between vehicle and PTH(7–34) treatments. Gene expression was evaluated using a similar a two-way ANOVA and post hoc tests. The relationship between lacuna size and CPR and MMR was tested using a Pearson correlation and linear regression, with a p-value < 0.05 representing a significant relationship.

Supplementary Material

Refer to Web version on PubMed Central for supplementary material.

Acknowledgments

This work was funded by the following sources: NIH DE07057 (DHK), AR056657 (DHK), AR064668 (JDG).

Abbreviations

(PTH)	Parathyroid Hormone
(MMR)	Mineral-to-Matrix Ratio
(CPR)	Carbonate-to-Phosphate Ratio

References

Akkus O, Adar F, Schaffler MB. Age-related changes in physicochemical properties of mineral crystals are related to impaired mechanical function of cortical bone. Bone. 2004; 34:443–453. [PubMed: 15003792]

Baig AA, Fox JL, Young RA, Wang Z, Hsu J, Higuchi WI, Chhettry A, Zhuang H, Otsuka M. Relationships among carbonated apatite solubility, crystallite size, and microstrain parameters. Calcif Tissue Int. 1999; 64:437–449. [PubMed: 10203421]

Blaber EA, Dvorochkin N, Lee C, Alwood JS, Yousuf R, Pianetta P, Globus RK, Burns BP, Almeida EA. Microgravity induces pelvic bone loss through osteoclastic activity, osteocytic osteolysis, and osteoblastic cell cycle inhibition by CDKN1a/p21. PloS one. 2013; 8:e61372. [PubMed: 23637819]

Bonewald LF. The amazing osteocyte. Journal of bone and mineral research: the official journal of the American Society for Bone and Mineral Research. 2011; 26:229–238.

Boskey A. Bone mineral crystal size. Osteoporosis Int. 2003; 14:S16–S20.

Boskey AL, Wright TM, Blank RD. Collagen and bone strength. Journal of bone and mineral research: the official journal of the American Society for Bone and Mineral Research. 1999; 14:330–335.

Britz HM, Carter Y, Jokihaara J, Leppanen OV, Jarvinen TL, Belev G, Cooper DM. Prolonged unloading in growing rats reduces cortical osteocyte lacunar density and volume in the distal tibia. Bone. 2012; 51:913–919. [PubMed: 23046687]

Burket J, Gourion-Arsiquaud S, Havill LM, Baker SP, Boskey AL, van der Meulen MC. Microstructure and nanomechanical properties in osteons relate to tissue and animal age. Journal of biomechanics. 2011; 44:277–284. [PubMed: 21074774]

Burstein AH, Zika JM, Heiple KG, Klein L. Contribution of collagen and mineral to the elastic-plastic properties of bone. The Journal of bone and joint surgery. American volume. 1975; 57:956–961.

Carden A, Rajachar RM, Morris MD, Kohn DH. Ultrastructural changes accompanying the mechanical deformation of bone tissue: a Raman imaging study. Calcif Tissue Int. 2003; 72:166–175. [PubMed: 12469250]

Clarke MV, Russell PK, Findlay DM, Sastra S, Anderson PH, Skinner JP, Atkins GJ, Zajac JD, Davey RA. A Role for the Calcitonin Receptor to Limit Bone Loss During Lactation in Female Mice by Inhibiting Osteocytic Osteolysis. Endocrinology. 2015; 156:3203–3214. [PubMed: 26135836]

de Carmejane O, Morris MD, Davis MK, Stixrude L, Tecklenburg M, Rajachar RM, Kohan DH. Bone chemical structure response to mechanical stress studied by high pressure Raman spectroscopy. Calcif Tissue Int. 2005; 76:207–213. [PubMed: 15742234]

Donnelly E, Boskey AL, Baker SP, van der Meulen MC. Effects of tissue age on bone tissue material composition and nanomechanical properties in the rat cortex. Journal of biomedical materials research. Part A. 2010; 92:1048–1056. [PubMed: 19301272]

Gadeleta SJ, Boskey AL, Paschalis E, Carlson C, Menschik F, Baldini T, Peterson M, Rimnac CM. A physical, chemical, and mechanical study of lumbar vertebrae from normal, ovariectomized, and nandrolone decanoate-treated cynomolgus monkeys (Macaca fascicularis). Bone. 2000; 27:541–550. [PubMed: 11033450]

Gardinier JD, Mohamed F, Kohn DH. PTH Signaling During Exercise Contributes to Bone Adaptation. Journal of bone and mineral research: the official journal of the American Society for Bone and Mineral Research. 2015; 30:1053–1063.

Hesse B, Langer M, Varga P, Pacureanu A, Dong P, Schrof S, Mannicke N, Suhonen H, Olivier C, Maurer P, Kazakia GJ, Raum K, Peyrin F. Alterations of mass density and 3D osteocyte lacunar

properties in bisphosphonate-related osteonecrotic human jaw bone, a synchrotron microCT study. PloS one. 2014; 9:e88481. [PubMed: 24586331]

Holmbeck K, Bianco P, Pidoux I, Inoue S, Billinghurst RC, Wu W, Chrysovergis K, Yamada S, Birkedal-Hansen H, Poole AR. The metalloproteinase MT1-MMP is required for normal development and maintenance of osteocyte processes in bone. Journal of cell science. 2005; 118:147–156. [PubMed: 15601659]

Hoshi A, Watanabe H, Chiba M, Inaba Y. Effects of exercise at different ages on bone density and mechanical properties of femoral bone of aged mice. Tohoku J Exp Med. 1998; 185:15–24. [PubMed: 9710941]

Huang TH, Lin SC, Chang FL, Hsieh SS, Liu SH, Yang RS. Effects of different exercise modes on mineralization, structure, and biomechanical properties of growing bone. J Appl Physiol. 2003; 95:300–307. [PubMed: 12611764]

Hui SL, Slemenda CW, Johnston CC Jr. Age and bone mass as predictors of fracture in a prospective study. The Journal of clinical investigation. 1988; 81:1804–1809. [PubMed: 3384952]

Iwamoto J, Shimamura C, Takeda T, Abe H, Ichimura S, Sato Y, Toyama Y. Effects of treadmill exercise on bone mass, bone metabolism, and calciotropic hormones in young growing rats. J Bone Miner Metab. 2004; 22:26–31. [PubMed: 14691683]

Iwamoto J, Yeh JK, Aloia JF. Differential effect of treadmill exercise on three cancellous bone sites in the young growing rat. Bone. 1999; 24:163–169. [PubMed: 10071907]

Iwasaki Y, Kazama JJ, Yamato H, Fukagawa M. Changes in chemical composition of cortical bone associated with bone fragility in rat model with chronic kidney disease. Bone. 2011; 48:1260–1267. [PubMed: 21397740]

Kelly NH, Schimenti JC, Patrick Ross F, van der Meulen MC. A method for isolating high quality RNA from mouse cortical and cancellous bone. Bone. 2014; 68:1–5. [PubMed: 25073031]

Kogawa M, Wijenayaka AR, Ormsby RT, Thomas GP, Anderson PH, Bonewald LF, Findlay DM, Atkins GJ. Sclerostin regulates release of bone mineral by osteocytes by induction of carbonic anhydrase 2. Journal of bone and mineral research: the official journal of the American Society for Bone and Mineral Research. 2013; 28:2436–2448.

Kohn DH, Sahar ND, Wallace JM, Golcuk K, Morris MD. Exercise Alters Mineral and Matrix Composition in the Absence of Adding New Bone. Cells Tissues Organs. 2009; 189:33–37. [PubMed: 18703871]

Maimoun L, Sultan C. Effect of Physical Activity on Calcium Homeostasis and Calciotropic Hormones: A Review. Calcified Tissue Int. 2009; 85:277–286.

McCreadie BR, Morris MD, Chen TC, Sudhaker Rao D, Finney WF, Widjaja E, Goldstein SA. Bone tissue compositional differences in women with and without osteoporotic fracture. Bone. 2006; 39:1190–1195. [PubMed: 16901772]

McNerny EM, Gardinier JD, Kohn DH. Exercise increases pyridinoline cross-linking and counters the mechanical effects of concurrent lathyrogenic treatment. Bone. 2015; 81:327–337. [PubMed: 26211995]

Morris MD, Mandair GS. Raman Assessment of Bone Quality. Clin Orthop Relat R. 2011; 469:2160–2169.

Nyman JS, Lynch CC, Perrien DS, Thiolloy S, O'Quinn EC, Patil CA, Bi X, Pharr GM, Mahadevan-Jansen A, Mundy GR. Differential effects between the loss of MMP-2 and MMP-9 on structural and tissue-level properties of bone. Journal of bone and mineral research: the official journal of the American Society for Bone and Mineral Research. 2011; 26:1252–1260.

Qing H, Ardeshirpour L, Pajevic PD, Dusevich V, Jahn K, Kato S, Wysolmerski J, Bonewald LF. Demonstration of osteocytic perilacunar/canalicular remodeling in mice during lactation. Journal of bone and mineral research: the official journal of the American Society for Bone and Mineral Research. 2012; 27:1018–1029.

Qing H, Bonewald LF. Osteocyte remodeling of the perilacunar and pericanalicular matrix. International journal of oral science. 2009; 1:59–65. [PubMed: 20687297]

Raghavan M, Sahar ND, Kohn DH, Morris MD. Age-specific profiles of tissue-level composition and mechanical properties in murine cortical bone. Bone. 2012; 50:942–953. [PubMed: 22285889]

Reilly GC. Observations of microdamage around osteocyte lacunae in bone. Journal of biomechanics. 2000; 33:1131–1134. [PubMed: 10854886]

Robling AG, Castillo AB, Turner CH. Biomechanical and molecular regulation of bone remodeling. Annual review of biomedical engineering. 2006; 8:455–498.

Sano H, Kikuta J, Furuya M, Kondo N, Endo N, Ishii M. Intravital bone imaging by two-photon excitation microscopy to identify osteocytic osteolysis in vivo. Bone. 2015; 74:134–139. [PubMed: 25624000]

Scott JPR, Sale C, Greeves JP, Casey A, Dutton J, Fraser WD. The role of exercise intensity in the bone metabolic response to an acute bout of weight-bearing exercise. J Appl Physiol. 2011; 110:423–432. [PubMed: 21127210]

Silver J, Naveh-Many T. FGF-23 and secondary hyperparathyroidism in chronic kidney disease. Nature reviews. Nephrology. 2013; 9:641–649. [PubMed: 23877588]

Tang SY, Herber RP, Ho SP, Alliston T. Matrix metalloproteinase-13 is required for osteocytic perilacunar remodeling and maintains bone fracture resistance. Journal of bone and mineral research: the official journal of the American Society for Bone and Mineral Research. 2012; 27:1936–1950.

Timlin JA, Carden A, Morris MD, Rajachar RM, Kohn DH. Raman spectroscopic imaging markers for fatigue-related microdamage in bovine bone. Analytical chemistry. 2000; 72:2229–2236. [PubMed: 10845368]

Wallace BA, Cumming RG. Systematic review of randomized trials of the effect of exercise on bone mass in pre- and postmenopausal women. Calcif Tissue Int. 2000; 67:10–18. [PubMed: 10908406]

Wallace JM, Golcuk K, Morris MD, Kohn DH. Inbred Strain-Specific Effects of Exercise in Wild Type and Biglycan Deficient Mice. Ann Biomed Eng. 2010; 38:1607–1617. [PubMed: 20033775]

Wallace JM, Ron MS, Kohn DH. Short-Term Exercise in Mice Increases Tibial Post-Yield Mechanical Properties While Two Weeks of Latency Following Exercise Increases Tissue-Level Strength. Calcified Tissue Int. 2009; 84:297–304.

Highlights

- Perilacunar tissue composition exhibited lower mineral density following exercise
- Endogenous PTH signaling during exercise mediated changes in tissue composition
- Perilacunar remodeling may explain corresponding changes in mechanical properties

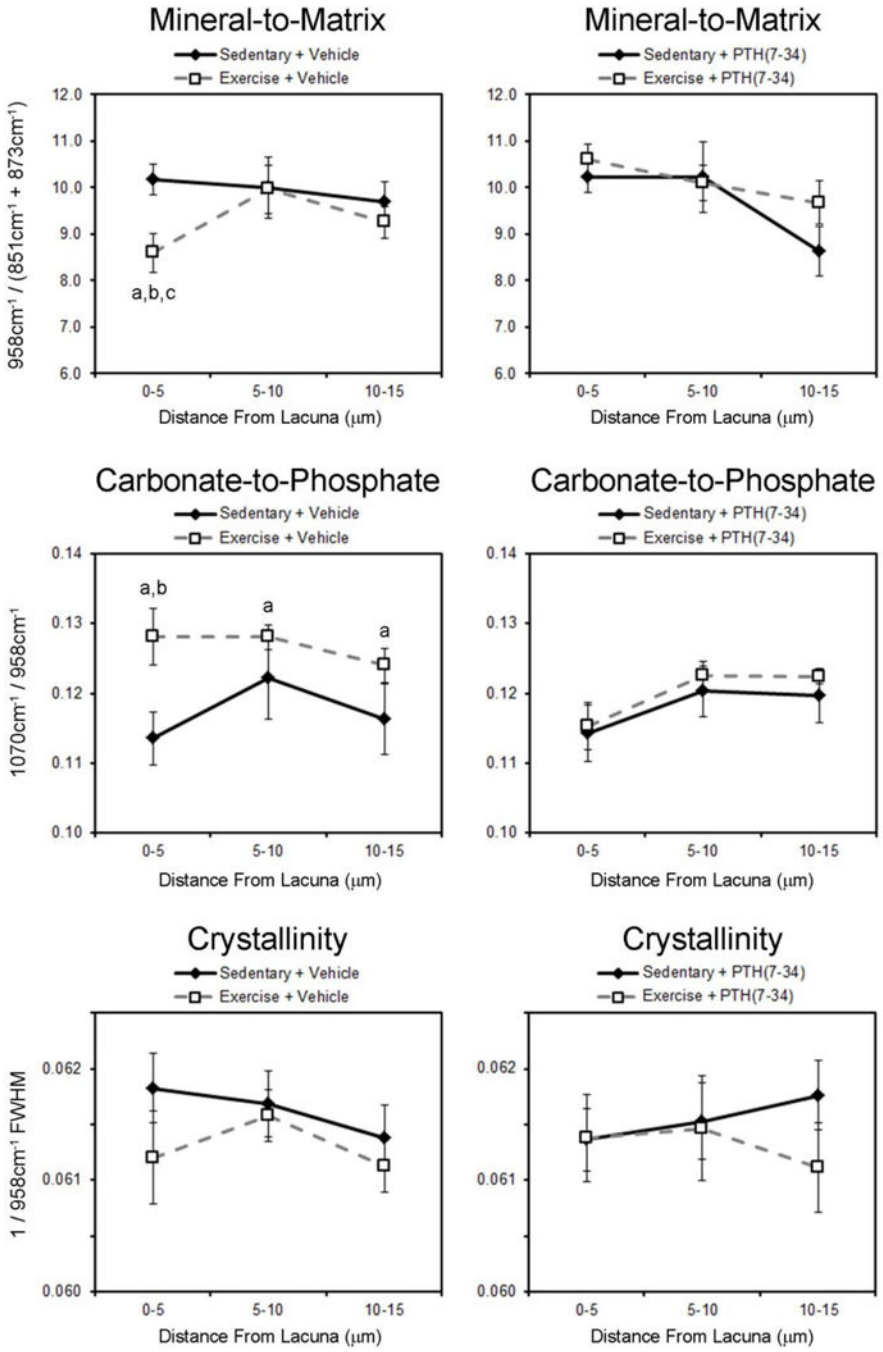

Figure 1. Perilacunar adaptation during exercise is evident by significantly decreased Mineral-to-Matrix Ratio (MMR) and significantly increased Carbonate-to-Phosphate Ratio (CPR), both of which were dependent on endogenous PTH signaling

Subscript ‘a’ indicates p-value < 0.05 between sedentary and exercise groups within the same region, ‘b’ indicates p-value < 0.05 between vehicle and PTH(7–34) treatment within the same region, ‘c’ indicates p-value < 0.05 between regions 0–5 and 5–10 within a single group and treatment. Power analysis of differences between sedentary and exercise was 0.835 with an alpha of 0.05. Mean ± SEM (n = 8, each n represents average of 3–4 images).

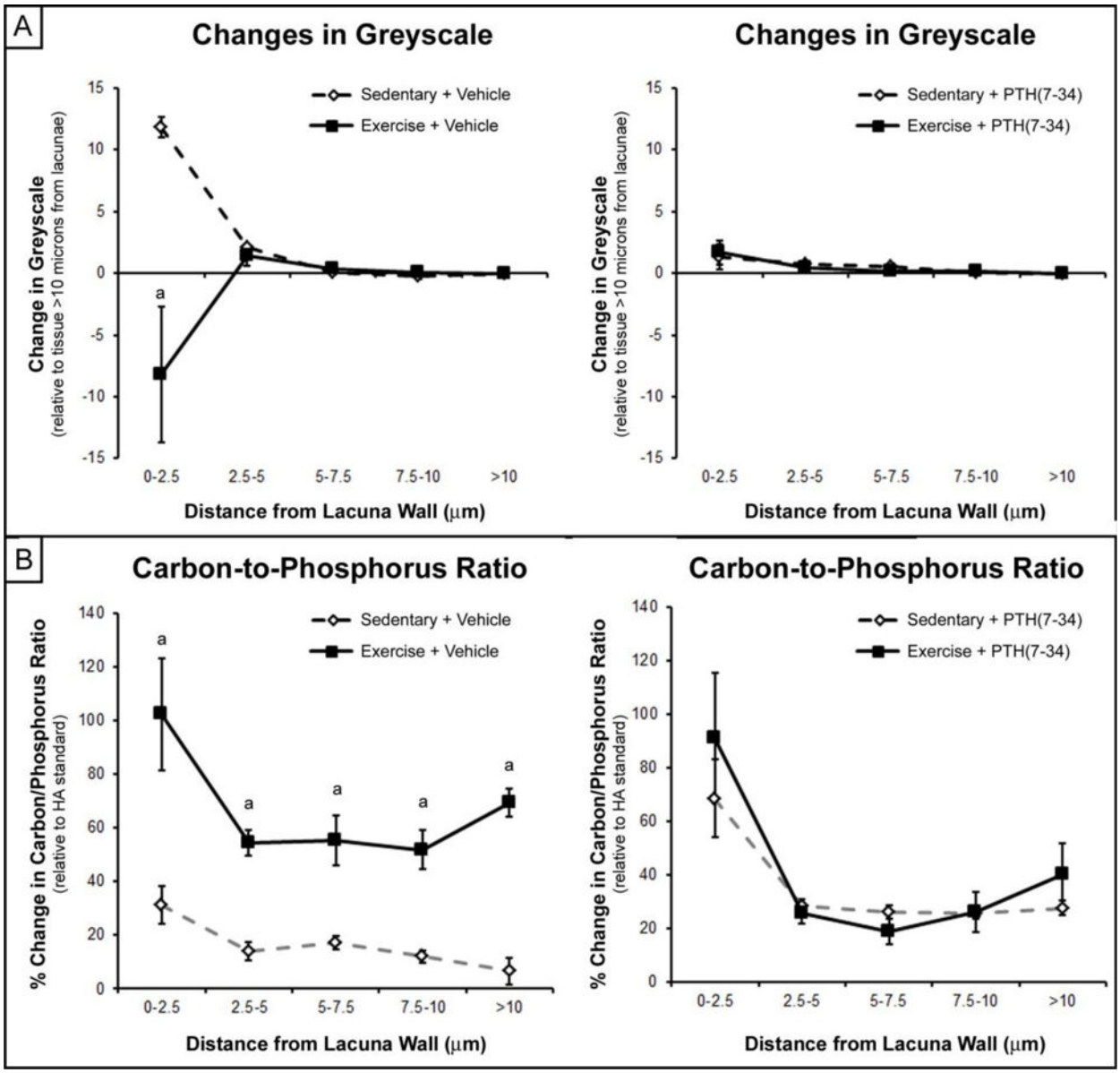

Figure 2. SEM and EDS confirmed the significant decrease in mineral content at the lacuna wall along with a significant increase in carbon content throughout the surrounding tissue

Subscript ‘a’ indicates p-value < 0.01 between exercise and sedentary measurements for a set distance from the lacuna wall. Displayed is the Mean ± SEM (n = 8, each n represents an average of 7 to 8 lacuna).

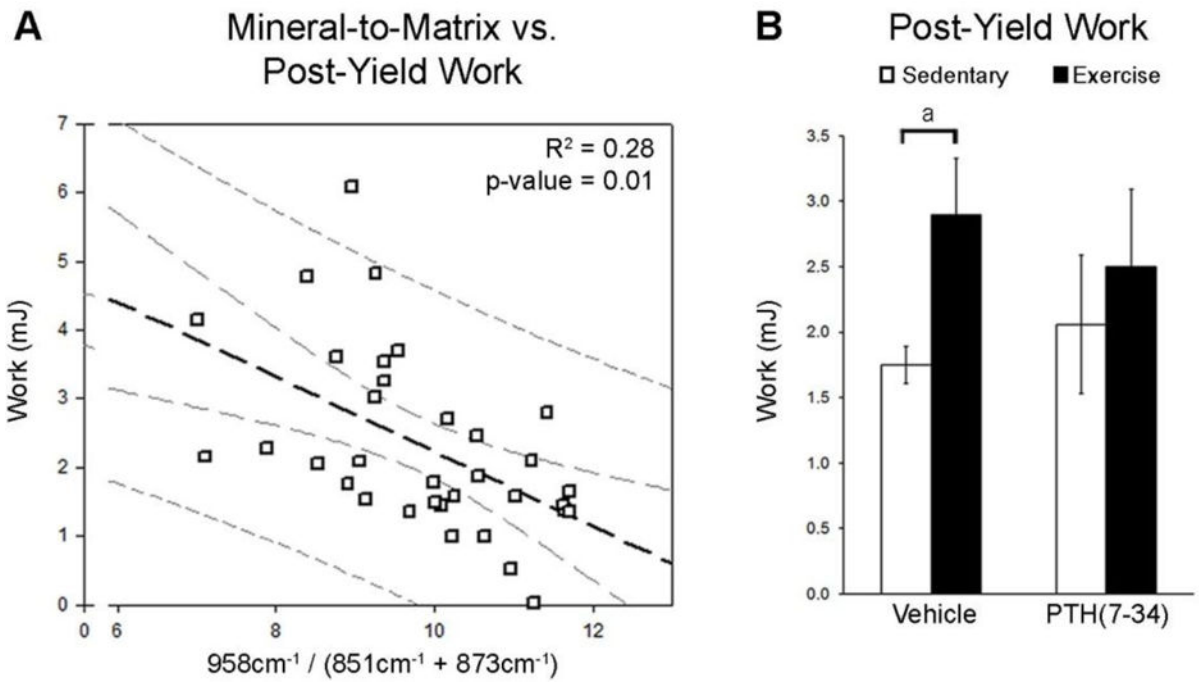

Figure 3. Post-yield work of the tibia demonstrated a significant negative correlation with the Mineral-Matrix Ratio (MMR) measured at the lacuna wall

A) Post-yield work exhibited a negative correlation with the perilacunar MMR (tissue within 0 to 5 microns of the lacuna wall). Linear regression is shown (black dashed line) with 95% confidence intervals (grey dashed line) and 95% prediction intervals (grey small dashed line). B) Among vehicle treated groups, exercise increased the post-yield work compared to sedentary controls, while PTH(7–34) treated groups displayed no significant difference. Displayed is the Mean ± SEM (n = 8).

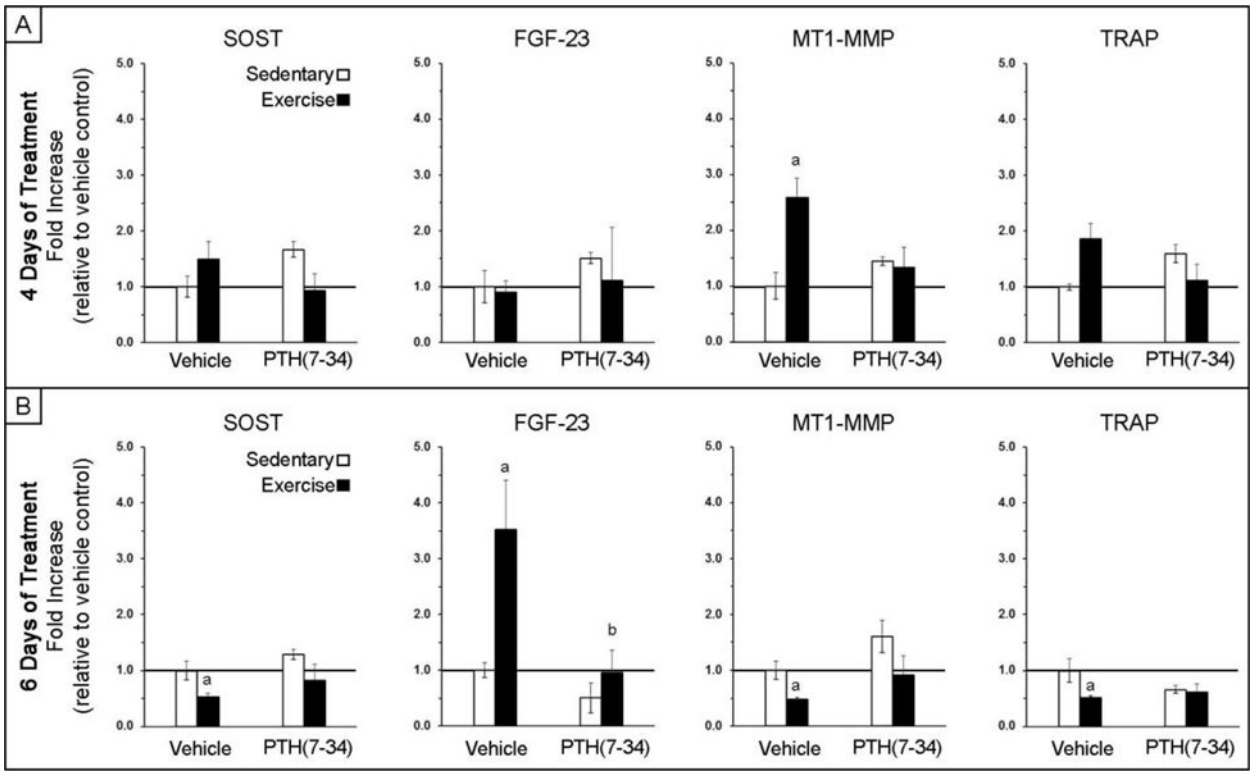

Figure 4. Gene expression in cortical bone revealed changes in tissue resorption and significantly increased osteocyte signaling during exercise

A) Each group was treated with exercise and/or PTH(7–34) for 4 days (A) or 6 days (B), after which gene expression within cortical bone was measured. By day 4, exercise increased MT1-MMP and TRAP expression. By day 6, exercise decreased MT1-MMP, TRAP, and SOST expression, but increased FGF-23 expression. Between PTH(7–34) treated groups, there were no significant changes in gene expression by day 4 or day 6. Based on paired t-test analysis, ‘a’ indicates p-value < 0.05 compared to sedentary control, ‘b’ indicates p-value < 0.05 compared to vehicle control (n = 4, each n represents tibias from 2 mice).

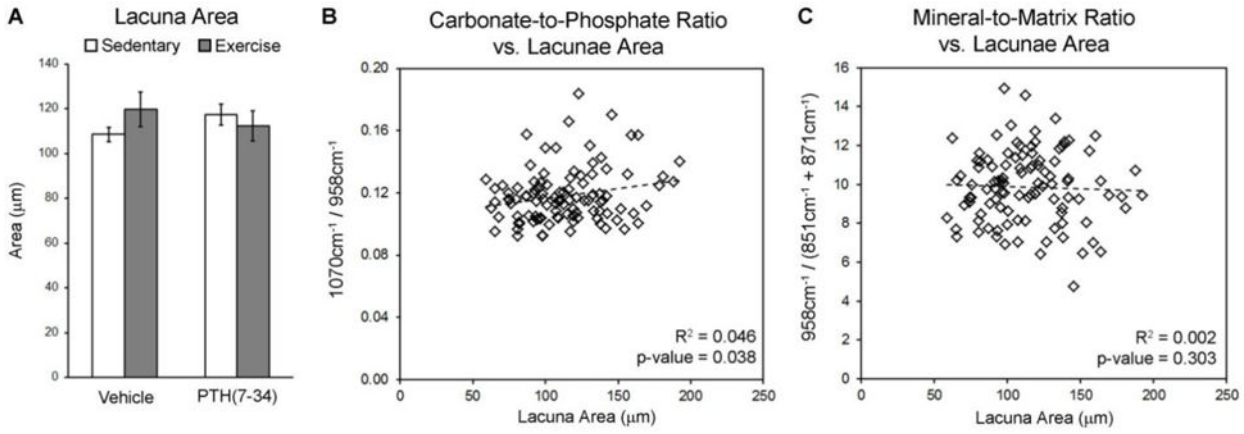

Figure 5. Perilacunar remodeling during exercise was accompanied by a non-significant increase in lacuna area, which correlated with an increase in CPR

Although lacuna area was greater following exercise (A), it was not statistically different from sedentary controls (p-value = 0.2). Lacuna area had a positive correlation with CPR (B), but did not correlate with MMR (C). Each correlation was performed using samples pooled from all the groups. Mean ± SEM is displayed for lacuna area.

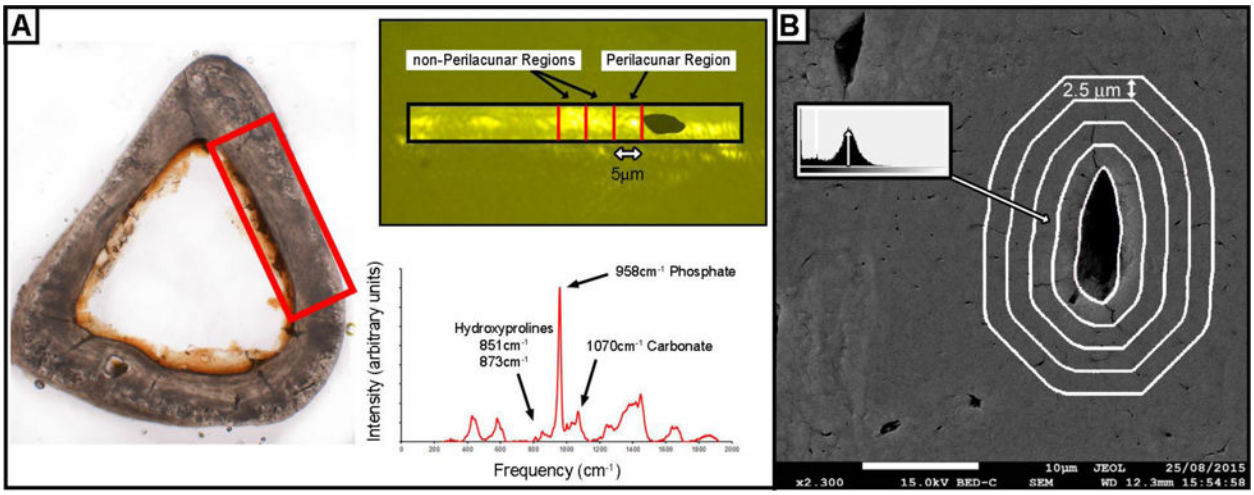

Figure 6. Raman spectra, SEM, and EDS analysis was performed around individual lacuna selected along the medial side of the tibia

A) The perilacunar region was defined as 0 to 5 microns away from the lacuna wall, while properties in non-perilacunar regions were measured in 5 micron increments in a zone 5–15 microns from the lacuna. B) For each BSE image the lacuna was outlined and then concentric outlines every 2.5 mm were identified. The mineral density in each region was defined as the grey-value of the histogram peak (inset).

Table 1

Both structural and tissue-level mechanical properties were increased by exercise, while only the structural-level properties were dependent on endogenous PTH signaling.

	Sedentary + Vehicle ave. (sem)	Exercise + Vehicle ave. (sem)	Sedentary + PTH(7–34) ave. (sem)	Exercise + PTH(7–34) ave. (sem)
Structural-level Properties				
Yield Displacement (mm)	260.3 (13.6)	208.0 (10.9)[a]	230.4 (6.3)	218.1 (6.7)
Yield Load (N)	18.06 (0.70)	17.63 (1.02)	17.01 (0.70)	17.11 (0.58)
Ultimate Displacement (mm)	278.1 (10.8)	251.9 (11.7)	279.2 (13.4)	254.5 (14.7)
Ultimate Load (N)	18.51 (0.62)	18.96 (1.08)	18.42 (0.73)	18.43 (0.73)
Stiffness (N/m)	81.40 (5.46)	99.91 (5.36)[a]	85.85 (3.03)	91.94 (2.50)
Failure Displacement (mm)	363.9 (12.5)	401.8 (40.8)	354.2 (29.2)	367.7 (28.8)
Failure Load (N)	15.74 (0.67)	14.49 (1.48)	16.03 (0.97)	15.73 (0.95)
Pre-Yield Work (mJ)	2.48 (0.19)	2.01 (0.20)	2.07 (0.11)	2.01 (0.12)
Post-Yield Work (mJ)	1.75 (0.14)	2.90 (0.43)[a]	2.06 (0.53)	2.50 (0.59)
Total Work (mJ)	4.23 (0.18)	4.91 (0.42)	4.13 (0.51)	4.51 (0.52)
Tissue-level Properties				
Yield Strain (με)	21126 (1062)	17201 (983)[a]	19174 (471)	17025 (641)[b]
Yield Stress (MPa)	175.89 (8.05)	184.40 (9.30)	172.27 (6.23)	183.55 (8.09)
Ultimate Strain (με)	22638 (987)	20896 (1233)	23302 (1323)	19964 (1436)
Ultimate Stress (MPa)	180.0 (6.9)	197.9 (8.9)[a]	186.8 (7.8)	197.2 (7.8)
Modulus (GPa)	9.65 (0.46)	12.68 (0.58)[a]	10.46 (0.40)	12.71 (0.68)[b]

[a] indicates p-value < 0.01 between vehicle treated sedentary and exercise groups,

[b] indicates p-value < 0.01 between PTH(7–34) treated sedentary and exercise groups (n = 8).

Table 2

The cross-sectional geometry and mineral density of the tibia were not affected by 3 weeks of exercise

The moment of inertia was derived about the anterior-posterior axis, while the distance to the neutral axis was measured from the most medial portion of the tibia since failure occurred along the medial side under tension. Each parameter was derived at the standard site located mid-way between the loading points of the mechanical testing (n = 8).

	Sedentary + Vehicle ave. (sem)	Exercise + Vehicle ave. (sem)	Sedentary + PTH(7–34) ave. (sem)	Exercise + PTH(7–34) ave. (sem)
Cortical Area (mm^2)	0.747 (0.020)	0.744 (0.190)	0.733 (0.022)	0.724 (0.013)
Distance to Neutral Axis (mm)	0.607 (0.008)	0.612 (0.013)	0.607 (0.011)	0.586 (0.010)
Moment of Inertia (mm^4)	0.093 (0.005)	0.088 (0.005)	0.088 (0.005)	0.082 (0.003)
Mineral Content (mg Ha)	1201.7 (7.7)	1200.5 (5.6)	1208.2 (6.6)	1220.7 (5.2)
Mineral Density (mg Ha/cm^2)	150.9 (4.3)	150.0 (4.0)	148.8 (4.7)	148.5 (3.1)